UC San Diego
UC San Diego Previously Published Works

Title
AMP-activated protein kinase activation ameliorates eicosanoid dysregulation in high-fat-induced kidney disease in mice

Permalink
https://escholarship.org/uc/item/3b6163nf

Journal
Journal of Lipid Research, 60(5)

ISSN
0022-2275

Authors
Declèves, Anne-Emilie
Mathew, Anna V
Armando, Aaron M
et al.

Publication Date
2019-05-01

DOI
10.1194/jlr.m088690

Peer reviewed

AMP-activated protein kinase activation ameliorates eicosanoid dysregulation in high-fat-induced kidney disease in mice[S]

Anne-Emilie Declèves,[1,2,*,†] Anna V. Mathew,[1,§] Aaron M. Armando,[**] Xianlin Han,[††] Edward A. Dennis,[**,§§] Oswald Quehenberger,[**,***] and Kumar Sharma*,[†††]

Institute of Metabolomic Medicine* and Departments of Pharmacology,** Chemistry and Biochemistry,§§ and Medicine,*** University of California, San Diego, La Jolla, CA; Laboratory of Metabolic and Molecular Biochemistry,† Faculty of Medicine, Université of Mons, Mons, Belgium; Division of Nephrology,§ Department of Internal Medicine, University of Michigan, Ann Arbor, MI; and Barshop Institute of Aging, Department of Medicine†† and Center for Renal Precision Medicine, Division of Nephrology, Department of Medicine,††† University of Texas Health San Antonio, San Antonio, TX

ORCID ID: 0000-0002-0838-2432 (A-E.D.)

Abstract High-fat diet (HFD) causes renal lipotoxicity that is ameliorated with AMP-activated protein kinase (AMPK) activation. Although bioactive eicosanoids increase with HFD and are essential in regulation of renal disease, their role in the inflammatory response to HFD-induced kidney disease and their modulation by AMPK activation remain unexplored. In a mouse model, we explored the effects of HFD on eicosanoid synthesis and the role of AMPK activation in ameliorating these changes. We used targeted lipidomic profiling with quantitative MS to determine PUFA and eicosanoid content in kidneys, urine, and renal arterial and venous circulation. HFD increased phospholipase expression as well as the total and free pro-inflammatory arachidonic acid (AA) and anti-inflammatory DHA in kidneys. Consistent with the parent PUFA levels, the AA- and DHA-derived lipoxygenase (LOX), cytochrome P450, and nonenzymatic degradation (NE) metabolites increased in kidneys with HFD, while EPA-derived LOX and NE metabolites decreased. Conversely, treatment with 5-aminoimidazole-4-carboxamide-1-β-D-furanosyl 5′-monophosphate (AICAR), an AMPK activator, reduced the free AA and DHA content and the DHA-derived metabolites in kidney. Interestingly, kidney and circulating AA, AA metabolites, EPA-derived LOX, and NE metabolites are increased with HFD; whereas, DHA metabolites are increased in kidney in contrast to their decreased circulating levels with HFD. Together, these changes showcase HFD-induced pro- and anti-inflammatory eicosanoid dysregulation and highlight the role of AMPK in correcting HFD-induced dysregulated eicosanoid pathways.—Declèves, A-E., A. V. Mathew, A. M. Armando, X. Han, E. A. Dennis, O. Quehenberger, and K. Sharma. **AMP-activated protein kinase activation ameliorates eicosanoid dysregulation in high-fat-induced kidney disease in mice.** *J. Lipid Res.* 2019. 60: 937–952.

Supplementary key words obesity • chronic kidney disease • high-fat diet • adenosine 5′-monophosphate-activated protein kinase • AICAR • adenosine 5′-monophosphate

The prevalence of obesity has continued to rise over the past few decades and was 36.5% among US adults between the years 2011 and 2014 (1). Obesity serves as a significant

risk factor for both the initiation and progression of kidney disease independent of hypertension and diabetes (2–4). Excessive intake of calorie-dense lipids leads to organ dysfunction both by direct lipotoxicity and inflammation. In fact, the Western diet enriched in saturated animal fats has been shown to increase albuminuria and cause a faster decline in renal function (5). In our previous studies, we established that high-fat diet (HFD)-induced kidney disease is characterized by renal hypertrophy, increased albuminuria, and elevated markers of renal fibrosis and inflammation (6). These HFD-induced markers of inflammation, oxidative stress, and fibrosis are reversed by AMP-activated protein kinase (AMPK) activation (6, 7).

HFD alters the activity of the crucial lipid metabolism enzymes, acetyl-CoA carboxylase (ACC) and HMG-CoA reductase (HMGCR), contributing to lipid accumulation in the kidney (6). Total cholesterol esters and phosphatidylcholine content in the kidney are elevated, while the FA and triglyceride content is unchanged. Phospholipid accumulation in the proximal tubules is associated with lysosomal dysfunction, stagnant autophagic flux, mitochondrial dysfunction, and inflammasome activation (8). High-fat feeding for long periods causes recruitment of macrophages, switch to macrophage pro-inflammatory phenotype, and increased inflammatory mediators like TNFα, monocyte chemoattractant protein-1 (MCP-1), IL-6, cyclooxygenase (COX)-2, and IL-1β (9–12). Diets rich in PUFAs are known to change plasma lipids, renal phospholipid content, and, subsequently, PUFA-derived eicosanoid inflammation in a rat model of nephrotic syndrome (13). However, the influence of renal eicosanoid synthesis and eicosanoid-derived inflammation in HFD-induced kidney disease is unknown.

Eicosanoids are oxylipins derived from arachidonic acid (AA) or related PUFAs and are inextricably related to inflammation in the kidney. The primary PUFAs for the *n-6* series and *n-3* series, linoleic acid (LA) and α-linolenic acid (ALA), respectively, are both derived from the diet. These 18-carbon PUFAs are then metabolized by various desaturase and elongase enzymes in a stepwise fashion. However, both LA and ALA are acted on by the same enzymes, resulting in a competition between the *n-3* and *n-6* series (14). LA is metabolized through multiple steps to dihomo-γ-linolenic acid (DGLA; 20:3n6) and, ultimately, to AA (20:4n6). On the other hand, ALA is metabolized to EPA (20:5 n-3) and subsequently to DHA (22:6 n-3) (15). These PUFAs are incorporated into membrane phospholipids and released by phospholipase A2 (PLA2) under the influence of various stimuli. In subsequent reactions, COXs, lipoxygenases (LOXs), and cytochrome P450 (P450) enzymes act on free PUFAs to form eicosanoids. Some eicosanoids can also be formed from PUFAs via nonenzymatic reactions [nonenzymatic degradation (NE)], e.g., isoprostanes.

Eicosanoids play an essential role in the regulation of renal physiology and disease by modulating renal blood flow, glomerular filtration rate, autoregulation, tubular glomerular feedback, excretion of renal water and sodium, and release of renin and erythropoietin. HFD feeding causes an increase in circulating eicosanoids. In the kidney, these eicosanoids are produced by all different cell types: mesangial cells, renal microvessels, and tubular cells. This makes it difficult to pinpoint the actual origin of these autacoids without actual profiling of the various compartments. Local production in the kidney will be reflected in the kidney tissue, renal venous compartment, and urine. Recent advances in eicosanoid analysis using highly sensitive MS have enabled us to profile over 150 different eicosanoid metabolites reliably in all tissues, enabling us to systematically profile the changes in the metabolic pathways with HFD and 5-aminoimidazole-4-carboxamide-1-β-D-furanosyl 5′-monophosphate (AICAR) therapy.

AMPK is a ubiquitous heterotrimeric kinase that acts as a cellular energy sensor that responds to changes in the intracellular AMP/ATP ratio (16). AICAR acts as a specific AMPK agonist (17). AMPK activation leads to inhibition of energy-requiring biochemical processes, like FA synthesis, and stimulation of energy-producing biochemical pathways, like β-oxidation, to improve energy efficiency (18). Metabolic stress, such as diabetes or obesity, impairs the activity of AMPK, and AMPK activation reduces the initial and sustained inflammatory response in the kidney of the HFD-induced kidney disease model (6). Along with lipid accumulation, the markers of inflammation were modulated with AICAR use (7). AMPK signaling has been shown to influence the secretory PLA2 expression in vascular smooth muscle cells (19) and control triglyceride content in adipocytes (20). AMPK activation also decreases the formation of 15-LOX metabolites of AA in macrophages (21). While AMPK activation is beneficial in lipid and eicosanoid metabolism in other tissues, the effect of HFD and AMPK activation on eicosanoid pathways in the kidney is unknown. We hypothesized that the high-fat exposure triggers inflammation involving the eicosanoid pathway and that eicosanoid production is ameliorated with AMPK activation. We used a targeted lipidomic platform to systematically investigate the HFD-associated eicosanoid synthesis induced in mice consuming HFD with or without AMPK activation in order to better understand the pathophysiological processes involved in HFD-induced kidney disease.

METHODS

Animals

All animal procedures were approved by the Institutional Animal Care and Use Committee of University of California, San Diego. Male 6-week-old C57BL/6 mice were purchased from Jackson Laboratory (Bar Harbor, ME) and fed either a standard diet (STD) [5% fat (PUFA, 2.1%; *n-6*, 1.9%; *n-3*, 0.2%), 24.5% protein, 40% carbohydrate] or a HFD [60% of total calories from fat (90% lard + 10% soybean oil; PUFA, 16.9%; *n-6*, 15.1%; *n-3*, 1.7%), 20% protein, 20% carbohydrate] (D12492; Research Diets, New Brunswick, NJ) for 14 weeks. The mice on the STD were treated with PBS and mice on HFD were treated with AICAR (0.5 mg/g body weight; Toronto Chemicals) or PBS via intraperitoneal injections for 5 days a week for a total of 14 weeks (6). Mice were placed in metabolic cages for 24 h urine collection before the start of the diets and after 14 weeks. Mice were euthanized after 14 weeks of diet, plasma was collected from the renal vein, and arterial blood

was obtained from direct cardiac puncture. After perfusion with PBS, kidneys were snap-frozen in liquid nitrogen for further analysis.

Quantitative total and free FA analysis

Total and free FAs were analyzed by GC-MS as previously described (22, 23). Briefly, kidney tissue (∼10 mg of tissue) was homogenized in 1 ml of PBS containing 10% methanol. For the analysis of total (esterified and free) FAs, kidney homogenates (50 μl) were spiked with deuterium-labeled FAs, acidified with 200 μl of 0.1 N hydrochloric acid, and extracted with 500 μl of methanol. Phase separation was achieved by the addition of 500 μl of dichloromethane (CH_2Cl_2), and the organic phase was removed. The extraction with dichloromethane was repeated, and the combined extracts were dried under argon gas. For saponification, the dried lipids were resuspended in 250 μl of methanol and 250 μl of 4 N potassium hydroxide, vortexed for 30 s, and incubated at 37°C for 1 h. The lipid hydrolysates were then neutralized with 260 μl of 4 N HCl and the free FAs were extracted twice with 2 ml of isooctane, and the combined extracts containing the hydrolyzed FAs were dried under argon before analysis with GC-MS.

Free FAs were extracted from 50 μl of the kidney tissue homogenates that were supplemented with a set of deuterated FAs that served as internal standards. The extraction was initiated by the addition of 25 μl of 1 N hydrochloric acid and 500 μl of methanol, and a biphasic solution was formed by the addition of 1 ml of isooctane. The isooctane phase containing the free FA fraction is removed, the extraction is repeated once more, and the combined extracts are dried under argon before analysis with the GC-MS.

In preparation for GC-MS analysis, the FAs (both total FA after saponification and free FA extracted from samples and the quantitative standards) were taken up in 25 μl of 1% diisopropylethylamine in acetonitrile and derivatized with 25 μl of 1% pentafluorobenzyl bromide. The FA esters were analyzed on an Agilent 6890N gas chromatograph equipped with an Agilent 5973 mass selective detector (Agilent, Santa Clara, CA) operated in the negative chemical ionization mode. Fatty acid quantitation was achieved by the stable isotope dilution method.

Quantitative eicosanoid analysis

Eicosanoids were analyzed by LC-MS, as described before (23, 24). For tissue analysis, eicosanoids were isolated from 0.9 ml of kidney homogenate supplemented with a set of internal standards consisting of 26 deuterated eicosanoids (Cayman Chemical) by solid phase extraction (Strata-X; Phenomenex, Torrance, CA) and eluted into 1 ml of methanol. For eicosanoid analysis in urine, 600 μl of sample were processed identically. The extracted samples were brought to dryness, reconstituted in 100 μL of LC buffer consisting of 63% water, 37% acetonitrile, and 0.02% formic acid, and a 40 μL aliquot was separated by reverse phase LC using a Synergy C18 column (2.1 × 250 mm, 4 μm; Phenomenex). Eicosanoids were analyzed using a tandem quadrupole mass spectrometer (MDS SCIEX 4000 Q Trap; Applied Biosystems, Foster City, CA) via scheduled multiple reaction monitoring in the negative ionization mode. Eicosanoids were identified in samples by matching the multiple reaction monitoring signal and LC retention times with those of pure standards. Data analysis was performed using MultiQuant 2.1 software (Applied Biosystems). Quantitative eicosanoid determination was performed using the stable isotope dilution method.

Immunoblot

Kidney tissue homogenates were electrophoretically separated on NuPAGE bis-Tris gels (Life Technologies) and transferred onto nitrocellulose membrane (Life Technologies). Antibodies to ELOLV5, cytosolic phospho-PLA2 and secretory PLA2 (Abcam), FADS1/FADS2 (Biorbyt, UK), and actin (Sigma) were used on the blots. Detection was performed with ECL Plus detection reagents (GE Healthcare) after treatment with appropriate secondary antibodies.

Statistical analysis

Results are presented as mean values ± SD. The kidney values were normalized with tissue weight and plasma values were normalized to volume. Urinary metabolites are all normalized to urine creatinine values. All metabolites were log transformed and auto-scaled before undergoing statistical analysis using the MetaboAnalyst version 3.0 software (25). Figures were generated using GraphPad Prism software version 4.03 . The difference between data groups was evaluated for significance using two-way ANOVA and Fisher's least significant difference method post hoc tests for multiple comparisons. A *P*-value less than 0.05 was defined as statistically significant in the non-MS experiments. To account for multiple comparisons with a large number of lipid metabolites, a false discovery rate (FDR; q value) of <0.05 was considered statistically significant. The highly correlated metabolites derived from a single enzyme pathway from a specific parent FA in each tissue compartment and then were separately aggregated into one secondary variable representative of the corresponding pathway using principal component (PC) analysis. We have then used the PC explaining the highest variance in the variable for further analysis to detect trends using SPSS version 25 (IBM Corp.) (26).

RESULTS

HFD increased phospholipase expression and free levels of PUFAs, and this action is reversed by AMPK activation

Both cytosolic and secretory PLA2 act on membrane phospholipids to release PUFAs, the precursors of various eicosanoids. Levels of cytosolic phospho-PLA2 (group IV) and secretory PLA2 were both increased with HFD in the kidney, and AICAR treatment decreased their levels (**Fig. 1**).

Targeted lipidomic analysis using MS of kidney tissue revealed unique patterns in the total and free ω3 and ω6 PUFA series that are demonstrated in **Fig. 2**. The total FA (esterified and unesterified FA) and free FA (unesterified) profiles generated from the kidney of mice fed a low-fat standard chow (STD), HFD, or HFD with the AMPK activator AICAR (HFD+AICAR) are displayed in supplemental Table S1. The total EPA and free EPA are decreased in the kidneys with the HFD (Fig. 2A, B; $P < 0.05$) and further decreased with AICAR, while both total DHA and free DHA (an *n-3* FA similar to EPA) are increased with HFD and reversed with the use of AICAR (Fig. 2C, D; $P < 0.05$). While DHA and EPA levels are modulated with HFD, the parent PUFA, ALA (total and unesterified), is unchanged.

The free and total *n-6* FA, DGLA, is decreased in the kidney with HFD, but unchanged with AICAR (Fig. 2E, F). Total AA and free AA in the kidney are increased by HFD, and the free AA decreased with AICAR (Fig. 2G, H). Free and total levels of LA, the precursor for both DGLA and AA, are unchanged by the diet and AICAR in the kidney. Delta-6
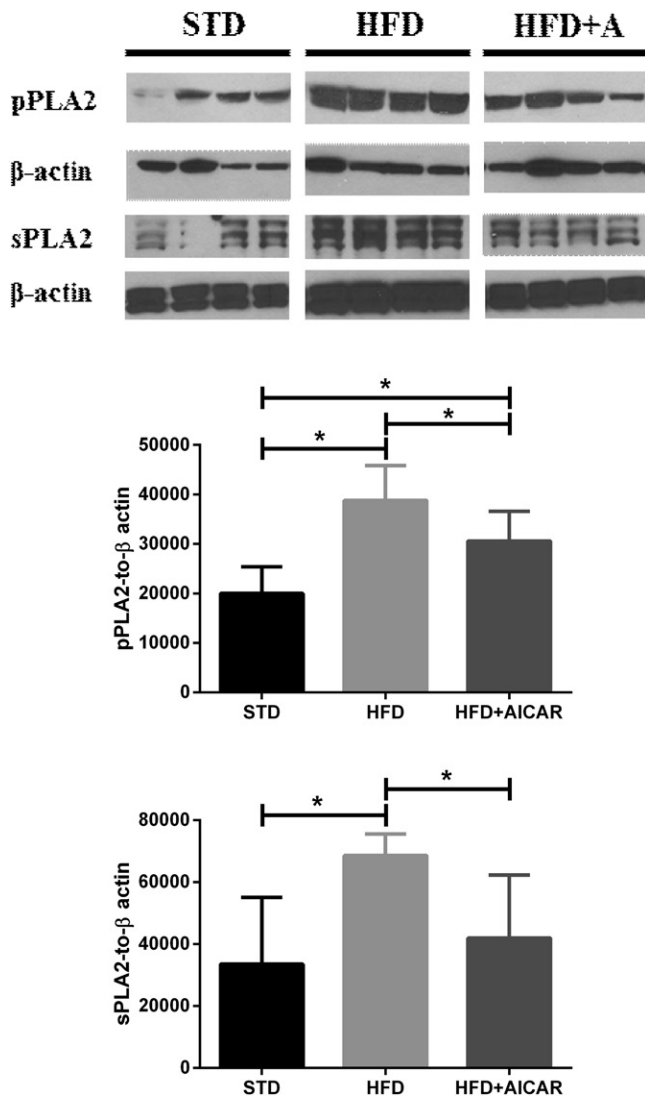
Fig. 1. HFD increases cytosolic PLA2 and secretory PLA2 (sPLA2) levels in the mouse kidney that are improved with AICAR treatment. Western blot analysis of the effect of STD, HFD, and HFD with AICAR (HFD+AICAR) treatment on cytosolic phospho-PLA2 (pPLA2) and sPLA2 in mouse kidney. Relative densitometry of the immunoblots was normalized with β-actin. Values are expressed as mean ± SD (n = 5 in each group). *$P < 0.05$.

desaturase and delta-5 desaturase catalyze desaturations at specific positions of FA substrates. Elongases extend the FA carbon chains by two carbons. The levels of both desaturases were not different between the three groups (supplemental Fig. S1).

HFD dysregulates kidney eicosanoid metabolism that is ameliorated by AMPK activation

The eicosanoid metabolites of AA, DHA, and EPA are regulated with HFD in the kidney (**Table 1**), and specific metabolites are modulated with AICAR (**Fig. 3**). HFD seems to create a clear increase in COX products of AA in the kidney and a decrease in COX products of EPA. 12-Hydroxyl-hexadecatrienoic acid, which is a COX/P450 product, is increased with HFD and decreased with AICAR (Fig. 3A). The P450 products of DHA, 16,17-

epoxy-docosapentaenoic acid (EpDPE) and its product 16-hydroxy-docosahexaenoic acid (HDoHE) and 19,20-EpDPE and its product 19,20-dihydroxy-docosapentaenoic acid (DiHDPA), are increased with HFD, but only the end products 19,20-DiHDPA and 16-HDoHE are decreased with AICAR (Fig. 3B, C). The LOX products of DHA (HDo-HEs), 4-HDoHE, 7-HDoHE, 11-HDoHE, and 17-HDoHE and its product, 15(t)-protectin D_1 (PD_1), are increased with HFD (Fig. 3D–F). NE products of DHA, 8-HDoHE, 10-HDoHE, 13-HDoHE, and 20-HDoHE, are increased with HFD and decreased with AICAR (Fig. 3G, 3H).

HFD and AMPK activation alter the urinary eicosanoid profiles

HFD-induced changes in urine metabolites are illustrated in **Table 2** and the metabolites that are altered with AICAR in **Fig. 4**. The overall trend of the kidney continues in the urine with a predominant increase of COX products of AA in the urine and a decrease of COX products of EPA. Adrenic acid and its COX metabolite, dihomo-prostaglandin (PG)$F_{2\alpha}$ (dihomo-$PGF_{2\alpha}$), are both increased with HFD in the urine, but only dihomo-$PGF_{2\alpha}$ is decreased with AICAR (Fig. 4A). Dihomo-15-deoxy-PGD_2 (dihomo-15d-PGD_2), which is a NE byproduct of another adrenic acid COX metabolite, is decreased with HFD and increased with AICAR (Fig. 4B).

Urine AA (Fig. 4C) is increased with HFD and decreased with AICAR, which is consistent with the trend in the kidney. Downstream COX metabolites of AA and PGH_2 are altered with the HFD and AICAR. The P450 metabolite of PGE_2, 13,14-dihydro-15-keto-PGE_2 (PGEM; Fig. 4D), is increased with HFD and decreased with AICAR. Another PGH_2 metabolite, 13,14-dihydro-5-keto-$PGF_{2\alpha}$ (PGFM; Fig. 4E), and $PGF_{2\alpha}$ (Fig. 4F), both the products of COX, are increased with HFD and decreased with HFD with AICAR. The PGD_2 metabolite, PGJ_2, is increased with HFD, while urinary 13,14-dihydro-15-keto-PGD_2 (dhk-PGD_2; Fig. 4G) both COX metabolites of AA is increased with HFD and decreased with HFD with AICAR. Similarly, the 5-iso-$PGF_{2\alpha}$-VI (5-iso-$PGF_{2\alpha}$-VI) (Fig. 4H), which is an NE product of AA, is increased with HFD and decreased with AICAR. PGE_3, an EPA metabolite of COX action, is increased with HFD and decreased with AICAR (Fig. 4I). The COX metabolite of EPA, thromboxane (TX)B_3, is decreased with HFD and increased with AICAR (Fig. 4J).

HFD and AMPK activation modulate circulating eicosanoid levels

In order to delineate the origin of the eicosanoids in the kidney, both the renal artery (**Table 3**) and vein (**Table 4**) were sampled after the mice were fed STD, HFD, and HFD with AICAR. The eicosanoid profile of the arterial and venous samples revealed that AA and its metabolite, 8,9-epoxyeicosatrienoic acid (EET) (a product of P450), were both increased with HFD. 5,6-EET and 11,12-EET are increased in the venous circulation, but not in the arterial circulation. Because these metabolites are also elevated in the kidney, this suggested the possible production of the metabolites in the kidney and release into the venous circulation.
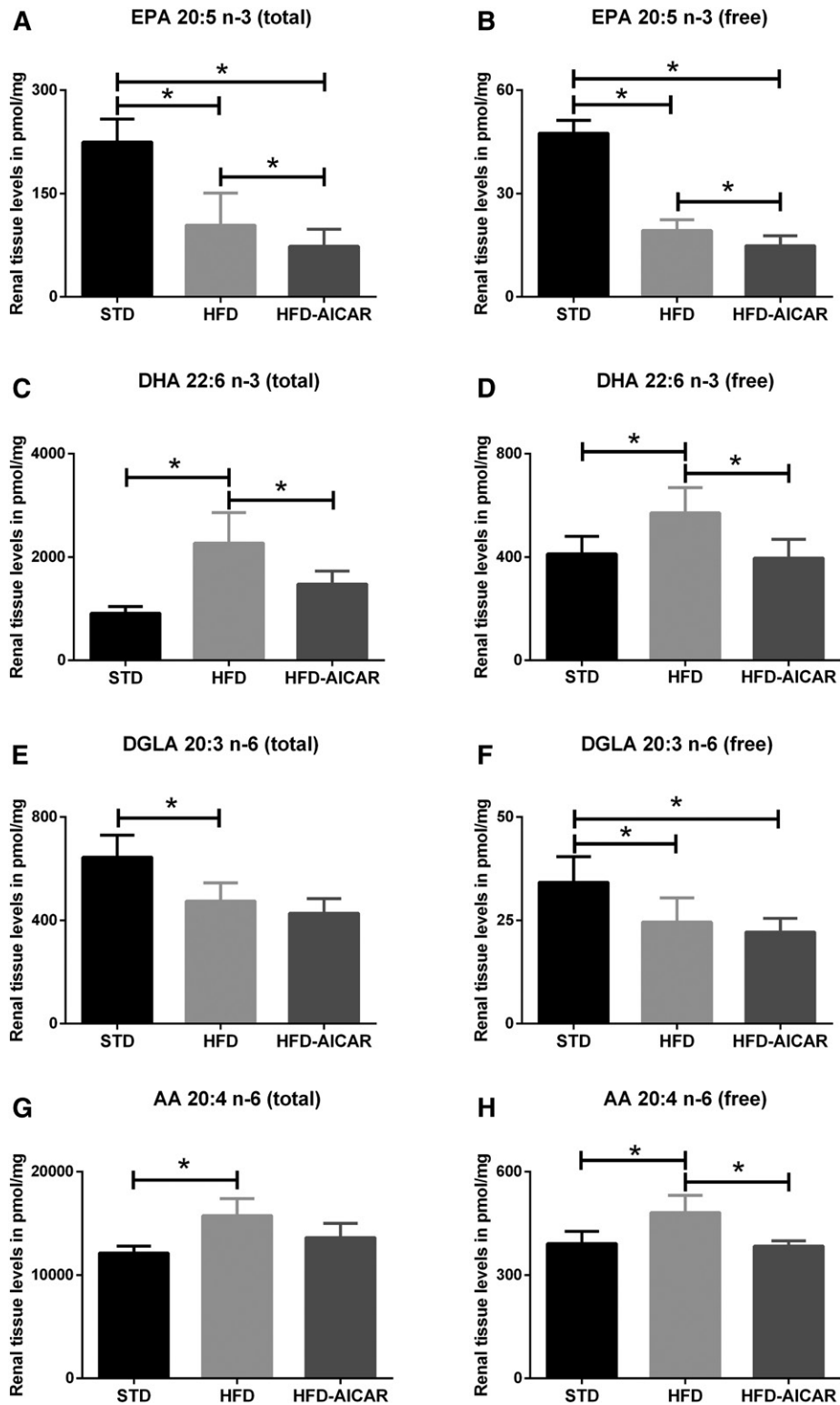
Fig. 2. HFD increases total and free PUFA levels in the mouse kidneys that are rescued by AMPK activation. Total and free levels of ω3 EPA (A, B) and DHA (C, D), and ω6 DGLA (E, F) and AA (G, H), in the mice fed STD, HFD, and HFD+AICAR. Values are expressed as mean ± SD (n = 6 in each group). *$P < 0.05$.

AA COX metabolite, 6-keto-PGF$_{1\alpha}$, is elevated in the venous circulation with HFD; this is in line with the elevation of the downstream metabolite, 6-keto-PGE$_1$, in the urine.

The DHA metabolites, 20-HDoHE, 10-HDoHE, and 13-HDoHE (products of NE), are all decreased in the venous circulation. 11-HDoHE and 4-HDoHE, products of the LOX pathway, and the 16-HDoHE, a product of P450, are all decreased with HFD in the venous circulation. 4-HDoHE and 20-HDoHE are also decreased with HFD in the arterial circulation.

TABLE 1. Eicosanoid metabolites altered with HFD in the kidney

Name	Acronym	MECH	STD	HFD	P	q Value
Up with HFD						
AA metabolites						
Arachidonic acid	AA	PUFA	243.4 ± 19.2	312.7 ± 40.9	0.010	0.037
13,14-Dihydro-15-keto-prostaglandin D_2	dhk-PGD_2	COX	0.04 ± 0.01	1.20 ± 0.02	0.008	0.035
5,6-Epoxyeicosatrienoic acid	5,6-EET	P450	1.59 ± 0.74	8.64 ± 5.64	0.014	0.045
11,12-Epoxyeicosatrienoic acid	11,12-EET	P450	0.02 ± 0.01	0.18 ± 0.13	0.015	0.045
5-Oxo-eicosatetraenoic acid	5-oxoETE	LOX	0.22 ± 0.11	1.56 ± 1.21	0.013	0.043
6(R),15(R)-lipoxin A_4	6(R),15(R)-LXA_4	LOX	0.02 ± 0.01	0.05 ± 0.02	0.006	0.032
6(S)-lipoxin A_4	6SLXA_4	LOX	0.02 ± 0.01	0.05 ± 0.02	0.015	0.045
9-Hydroxy-eicosatetraenoic acid	9-HETE	NE	0.02 ± 0.01	0.14 ± 0.09	0.013	0.043
DHA metabolites						
16,17-Epoxy-docosapentaenoic acid	16,17-EpDPE	P450	0.42 ± 0.07	0.65 ± 0.08	0.001	0.010
16-Hydroxy-docosahexaenoic acid	16-HDoHE	P450	0.60 ± 0.07	1.20 ± 0.24	<0.001	0.003
19,20-Epoxy-docosapentaenoic acid	19,20-EpDPE	P450	1.03 ± 0.19	1.63 ± 0.22	0.001	0.010
19,20-Dihydroxy-docosapentaenoic acid	19,20-DiHDPA	P450	0.55 ± 0.10	1.32 ± 0.43	0.001	0.008
4-Hydroxy-docosahexaenoic acid	4-HDoHE	LOX	1.22 ± 0.20	3.17 ± 1.36	0.007	0.032
7-Hydroxy-docosahexaenoic acid	7-HDoHE	LOX	0.17 ± 0.02	0.32 ± 0.09	0.004	0.021
11-Hydroxy-docosahexaenoic acid	11-HDoHE	LOX	0.25 ± 0.03	0.45 ± 0.06	<0.001	0.001
17-Hydroxy-docosahexaenoic acid	17-HDoHE	LOX	1.04 ± 0.13	1.84 ± 0.31	<0.001	0.005
Protectin DX	PDX	LOX	0.02 ± 0.01	0.07 ± 0.02	0.009	0.037
15(t)-Protectin D_1	15(t)-PD_1	LOX	4.14 ± 0.89	12.68 ± 3.76	0.001	0.008
8-Hydroxy-docosahexaenoic acid	8-HDoHE	NE	0.67 ± 0.08	1.16 ± 0.24	0.001	0.009
10-Hydroxy-docosahexaenoic acid	10-HDoHE	NE	0.26 ± 0.03	0.45 ± 0.07	0.001	0.007
13-Hydroxy-docosahexaenoic acid	13-HDoHE	NE	0.51 ± 0.10	0.78 ± 0.11	0.003	0.017
20-Hydroxy-docosahexaenoic acid	20-HDoHE	NE	1.61 ± 0.22	2.46 ± 0.40	0.002	0.013
EPA metabolites						
11-Hydroxy-eicosapentaenoic acid	11-HEPE	NE	0.28 ± 0.10	2.0 ± 1.50	0.010	0.037
Down with HFD						
AA metabolites						
Prostaglandin E_2	PGE_2	COX	2.88 ± 1.02	1.43 ± 0.21	0.011	0.040
Dihomo-γ-LA metabolites						
15-Keto-prostaglandin $F_{1\alpha}$	15-keto-$PGF_{1\alpha}$	COX	0.43 ± 0.09	0.23 ± 0.08	0.007	0.032
15-Hydroxy-eicosatrienoic acid	15-HETrE	LOX	0.46 ± 0.07	0.34 ± 0.04	0.009	0.037
EPA metabolites						
5-Hydroxy-eicosapentaenoic acid	5-HEPE	LOX	0.24 ± 0.03	0.09 ± 0.02	<0.001	0.001
12-Hydroxy-eicosapentaenoic acid	12-HEPE	LOX	4.23 ± 0.31	1.17 ± 0.26	<0.001	<0.001
15-Hydroxy-eicosapentaenoic acid	15-HEPE	LOX	0.15 ± 0.02	0.05 ± 0.01	<0.001	<0.001
18-Hydroxy-eicosapentaenoic acid	18-HEPE	NE	0.22 ± 0.03	0.07 ± 0.01	<0.001	<0.001

All values are picomoles per milligram of renal tissue expressed as mean ± SD. MECH, mechanism.

EPA levels are decreased in both the arterial and venous circulation. EPA produces hydroxy-eicosapentaenoic acids (HEPEs), NE products; 18-HEPE, 11-HEPE, and 9-HEPE were decreased in the arterial and venous circulation. 5-HEPE, 12-HEPE, and 15-HEPE are produced from their respective LOXs and were decreased with HFD in both the arterial and venous circulation. 15-HEPE is decreased further with AICAR therapy in the arterial circulation. P450 metabolite, 14(15)-epoxyeicosatetraenoic acid [14(15)-EpETE], is decreased with HFD diet in both arterial and venous circulation and further with AICAR in the arterial circulation.

LA metabolites of P450, 9,10-dihydroxy-octadecanoic acid (diHOME), 12,13-diHOME, and 12,13-epoxy-octadecanoic acid (EpOME), are decreased with HFD and are increased with AICAR in the arterial circulation (**Fig. 5A**–C). Venous sampling revealed that 9-hydroxy-octatrienoic acid (9-HOTrE) (a product of LOX derived from ALA) is decreased with HFD, but increased with AICAR (Fig. 5D). 5-HEPE, a LOX metabolites of EPA, is decreased with HFD and increased with AICAR treatment (Fig. 5E).

Specific eicosanoids are altered by AMPK activation

When taken as a whole, there were significant changes in eicosanoid pathways in arterial and venous circulation,

urine, and kidney compartments (supplemental Table S2). **Figure 6** depicts the changes influenced by AICAR therapy on HFD mice. To further detect trends in the changes, the highly correlated eicosanoids derived from a parent PUFA and acted on by specific enzymatic pathways were collapsed into PCs and analyzed for trends and statistical significance. **Table 5** represents the trends in the kidney and urine of these highly correlated metabolites. In the kidney, HFD decreased EPA metabolites across all enzymatic pathways, while the COX metabolites alone were reversed by AICAR. Meanwhile, AA metabolites of urine were mostly elevated with HFD, whereas the COX EPA metabolites are decreased with HFD, and this is reversed with AICAR therapy. COX metabolites of adrenic acid are decreased with HFD in the urine and this was reversed with AICAR. **Table 6** reveals that EPA, DHA, and ALA metabolites were all decreased with HFD in the arterial and venous blood.

DISCUSSION

This is the first study to systematically explore the effects of HFD on eicosanoid synthesis in the kidney and the role of AMPK activation in ameliorating these changes. We find that HFD increases PLA2 expression and activity (through
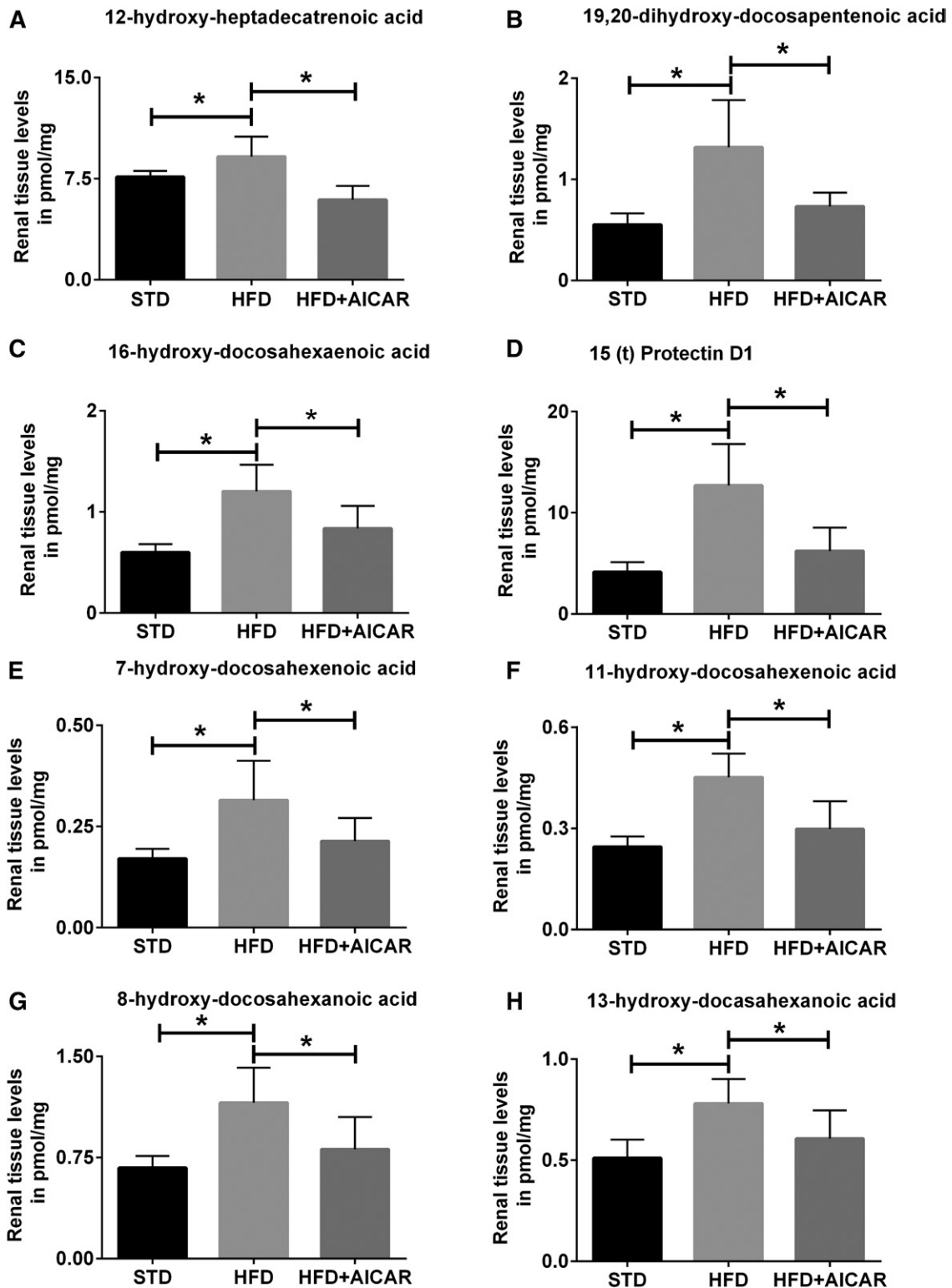
Fig. 3. Profile of eicosanoid species modulated by HFD and AMPK activation in mouse kidneys. Eicosanoid profiles show changes in the kidneys of mice fed STD, HFD, and HFD+AICAR. Values are expressed as mean ± SD (n = 6 in each group). Statistical analyses were performed by one-way ANOVA followed by Fisher post hoc tests. All *P* values corrected for Bonferroni FDR correction of *q ≤ 0.05. AA metabolite of P450, 12-hydroxyl-hexadecatrienoic acid) (A); DHA metabolites of P450, 19,20-dihydroxy-docosapenatenoic acid (19,20-DHDPA) (B) and 16-HDoHE (C); LOX metabolites, 15(t)-PD$_1$ (D), 7-HDoHE (E), and 11-HDoHE (F); and nonenzymatic process, 8-HDoHE (G) and 13-HDoHE (H).

phosphorylation) in the kidney that is largely corrected by AMPK activation. HFD increases both the pro-inflammatory AA and the anti-inflammatory DHA and their respective downstream products in the kidney and urine, and these changes are reversed with AICAR therapy. However, HFD decreases EPA, DGLA, LOX, and NE metabolites of EPA,

TABLE 2. Eicosanoid metabolites altered with HFD in the urine

| Name	Acronym	MECH	STD	HFD	P	q Value
Up with HFD						
Adrenic acid metabolites						
Adrenic acid	Adrenic acid	PUFA	0.018 ± 0.009	0.27 ± 0.27	0.001	0.011
Dihomo-prostaglandin $F_{2\alpha}$	dihomo-PGF$_{2\alpha}$	COX	0.009 ± 0.003	0.62 ± 0.18	<0.001	<0.001
AA metabolites						
Arachidonic acid	AA	PUFA	1.768 ± 0.619	14.7 ± 8.9	<0.001	0.003
Prostaglandin A_2	PGA$_2$	COX	0.018 ± 0.018	0.09 ± 0.03	0.001	0.0011
Prostaglandin B_2	PGB$_2$	COX	0.035 ± 0.009	0.09 ± 0.09	<0.001	0.005
13,14-Dihydro-15-keto-prostaglandin E_2	PGEM	COX	0.354 ± 0.035	1.23 ± 0.17	<0.001	<0.001
Prostaglandin J_2	PGJ$_2$	COX	0.002 ± 0.002	0.009 ± 0.004	0.002	0.017
13,14-Dihydro-15-keto-prostaglandin D_2	dhk-PGD$_2$	COX	0.008 ± 0.003	0.026 ± 0.004	<0.001	<0.001
6,15-Diketo-13,14-dihydro-prostaglandin $F_{1\alpha}$	6,15 dk-,dh-PGF$_{1\alpha}$	COX	0.27 ± 0.09	2.12 ± 0.79	<0.001	0.001
Prostaglandin $F_{2\alpha}$	PGF$_{2\alpha}$	COX	0.001 ± 0.001	0.09 ± 0.026	0.004	0.023
13,14-Dihydro-15- keto-prostaglandin $F_{2\alpha}$	PGFM	COX	1.59 ± 0.26	7.25 ± 1.76	<0.001	<0.001
6-Keto-prostaglandin E_1	6kPGE$_1$	COX	0.09 ± 0.009	0.09 ± 0.017	0.002	0.013
8,9-Dihydroxy-eicosatrienoic acid	8,9-diHETrE	P450	0.002 ± 0.0009	0.006 ± 0.0017	<0.001	0.001
11,12-Epoxyeicosatrienoic acid	11,12-EET	P450	0.002 ± 0.0009	0.005 ± 0.002	0.002	0.013
Eoxin D_4	EXD$_4$	LOX	20.69 ± 13.26	192.5 ± 69.2	<0.001	0.001
Eoxin E_4	EXE$_4$	LOX	0.088 ± 0.088	2.56 ± 1.6	0.009	0.045
5-Iso-prostaglandin $F_{2\alpha}$-VI	5-iso-PGF$_{2\alpha}$-VI	NE	0.026 ± 0.007	0.09 ± 0.09	<0.001	0.001
8-Iso-prostaglandin $F_{2\alpha}$	8-iso-PGF$_{2\alpha}$	NE	0.08 ± 0.009	0.17 ± 0.09	0.008	0.042
DHA metabolites						
Protectin DX	PDX	LOX	11.22 ± 13.96	27.5 ± 8.7	0.008	0.042
19,20-Dihydroxy-docosapentaenoic acid	19,20-DiHDPA	P450	0.009 ± 0.006	0.026 ± 0.017	0.009	0.046
EPA metabolites						
Prostaglandin E_3	PGE$_3$	COX	0.18 ± 0.09	3.62 ± 2.12	<0.001	0.000
LA metabolites						
9-Oxo-octadecadienoic acid	9-oxoODE	COX	2.39 ± 0.97	54.7 ± 2.1	0.001	0.011
Down with HFD						
EPA metabolites						
Prostaglandin D_3	PGD$_3$	COX	0.71 ± 0.26	0.17 ± 0.17	0.003	0.021
Prostaglandin $F_{3\alpha}$	PGF$_{3\alpha}$	COX	$73,739.8 \pm 35,060.9$	$18,813.4 \pm 15,625.1$	0.001	0.011
Thromboxane B_3	TXB$_3$	COX	0.044 ± 0.009	0.026 ± 0.009	0.008	0.042

All values are nanograms per milligram of creatinine expressed as mean ± SD. MECH, mechanism.

while AICAR therapy decreases free EPA levels further in the kidney. The P450 and NE metabolites of LA were decreased in the arterial circulation with HFD. This decrease was prevented with AICAR. These changes highlight the changes in eicosanoid pathways in the kidney with HFD that are ameliorated by AICAR therapy.

Obesity and metabolic syndrome patients have demonstrated altered FA and eicosanoid metabolism compared with lean subjects. Increased serum DGLA levels and low delta-5 desaturase activity were associated with hepatic steatosis over and above conventional risk factors in metabolic syndrome subjects (27). Like our HFD mouse model, COX, LOX, and P450 metabolites of AA and other PUFAs are elevated in the plasma of obese subjects compared with lean subjects (28). Increased TXA$_2$ can cause vasoconstriction and induce transcription of collagen in the glomerular matrix. In contrast, PGI$_2$ counteracts the deleterious TXA$_2$ effects associated with progressive glomerular damage by acting as a vasodilator. A decreased urinary PGI$_2$/TXA$_2$ ratio has been demonstrated in diabetic humans compared with controls (29). In the Japanese population, urinary 8-iso-PGF$_{2\alpha}$, which is an AA metabolite, predicts metabolic risks like obesity, hypertension, and glucose tolerance (30). Meanwhile, low serum lipoxin A4 levels (AA metabolite) are associated with metabolic syndrome risk in the Chinese population, similar to the elevated kidney levels of lipoxin A4 and its metabolite in our study (31).

Obesity-induced kidney disease is characterized by glomerular enlargement, podocyte loss, and proteinuria, eventually leading to renal failure (2, 32, 33). In animal models, HFD increased kidney weight and glomerular area with periodic acid-Schiff-positive matrix and increased Oil red-O-positive vacuolated cells. HFD also caused albuminuria, increased glomerular inflammation via the NFκB pathway, and increased urinary MCP-1 and hydrogen peroxide (6, 34). Increased fat intake increases kidney triglyceride content via increased SREBP-1 and -2 and lipogenesis along with reduced AMPK and increased ACC expression and activity in mice (7, 10, 35). Also, HFD decreased renal lipolysis along with carnitine palmitoyl acyl-CoA transferase-1 expression (36). Mice fed with HFD demonstrated vacuolization of the proximal tubule enriched with multi-lamellar lysosomal bodies with phospholipids the phenomenon was confirmed with human biopsies (37). Human studies have described the accumulation of ectopic lipid in obesity-induced kidney disease (4, 38). Mice lacking the innate immune receptor, Nlrp3, did not develop the pathological markers of HFD-induced kidney disease, indicating that pathways regulated by Nlrp3 could control the development of HFD-induced renal pathology (39). Clearly, HFD causes dysregulation of mainstream lipid metabolism in the kidney, but the gateway for many inflammatory mediator's eicosanoid generation with HFD has not been clearly examined.
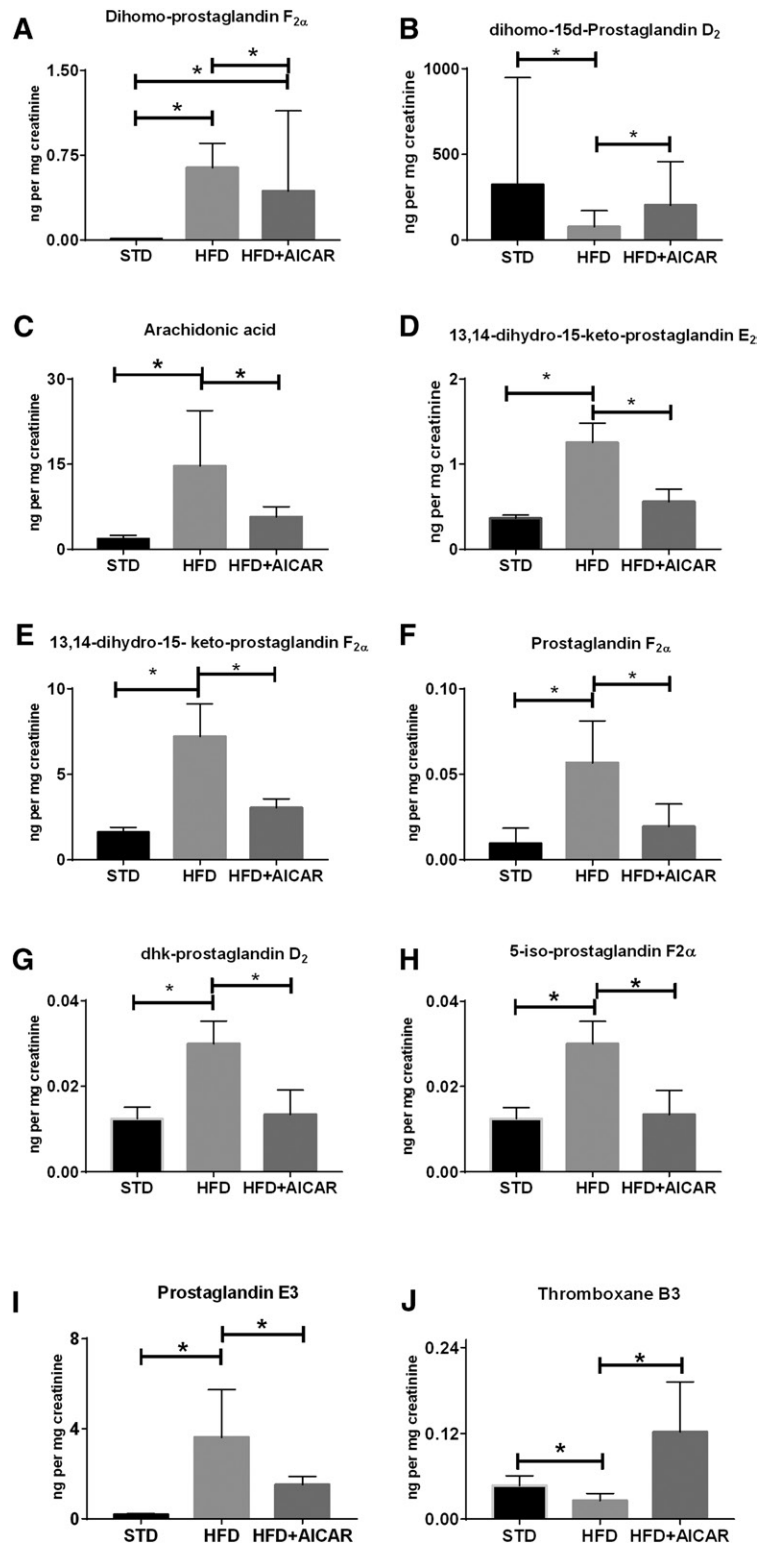
Fig. 4. Profile of urinary eicosanoid species in mice on HFD and AICAR (HFD+AICAR). Eicosanoid species in urine were normalized for concentration with creatinine levels in STD, HFD, and HFD with AICAR therapy. Values are expressed as the mean ± SD of original data or normalized data (log transformed, auto scaled) represented as box plots with whiskers (median, interquartile interval) (n = 6 in each group). Statistical analyses were performed by one-way ANOVA by Fisher post hoc tests. All *P* values corrected for Bonferroni FDR correction of *q ≤ 0.05. Adrenic acid metabolites, dihomo-$PGF_{2\alpha}$ (A) and dihomo-15d-PGD_2 (B). Urine AA (C) and its COX metabolites, PGEM (D), PGFM (E), $PGF_{2\alpha}$ (F), dhk-PGD_2 (G), and nonenzymatic product 5-iso-$PGF_{2\alpha}$-VI (H). COX metabolites of EPA, PGE_3 (I) and TXB_3 (J).

TABLE 3. Eicosanoid metabolites altered with HFD in the arterial circulation

Name	Acronym	MECH	STD	HFD	P	q Value
Up with HFD						
AA metabolites						
Arachidonic acid	AA	PUFA	8,771.3 ± 1,930.9	14,906.2 ± 2,726.5	0.002	0.011
8,9-Epoxy-eicosatrienoic acid	8,9-EET	P450	0.10 ± 0.14	3.77 ± 3.41	0.001	0.005
Down with HFD						
ALA metabolites						
9-Hydroxy-octatrienoic acid	9-HOTrE	LOX	2.97 ± 0.90	0.99 ± 0.31	<0.001	0.003
DHA metabolites						
4-Hydoxy-docosahexaenoic acid	4-HDoHE	LOX	8.93 ± 1.43	3.45 ± 0.91	<0.001	0.001
11-Hydoxy-docosahexaenoic acid	11-HDoHE	LOX	3.03 ± 1.13	1.35 ± 0.80	0.014	0.042
16-Hydoxy-docosahexaenoic acid	16-HDoHE	P450	1.49 ± 0.55	0.58 ± 0.17	0.002	0.012
10-Hydoxy-docosahexaenoic acid	10-HDoHE	NE	2.56 ± 0.92	1.05 ± 0.52	0.009	0.031
13-Hydoxy-docosahexaenoic acid	13-HDoHE	NE	3.62 ± 0.27	1.94 ± 0.81	0.010	0.035
20-Hydoxy-docosahexaenoic acid	20-HDoHE	NE	1.49 ± 0.62	0.11 ± 0.10	0.002	0.012
EPA metabolites						
EPA	EPA	PUFA	12,331.9 ± 4,377.1	4,870.6 ± 1,329.8	0.003	0.016
5-Hydroxy-eicosapentaenoic acid	5-HEPE	LOX	2.53 ± 0.28	0.38 ± 0.13	<0.001	0.000
12-Hydroxy-eicosapentaenoic acid	12-HEPE	LOX	33.76 ± 22.64	4.46 ± 3.22	0.004	0.018
15-Hydroxy-eicosapentaenoic acid	15-HEPE	LOX	1.65 ± 0.45	0.20 ± 0.13	0.004	0.018
14(15)-Epoxy-eicosatetraenoic acid	14,15-EpETE	P450	0.56 ± 0.18	0.18 ± 0.05	<0.001	0.004
9-Hydroxy-eicosapentaenoic acid	9-HEPE	NE	3.56 ± 1.84	0.11 ± 0.13	<0.001	0.003
11-Hydroxy-eicosapentaenoic acid	11-HEPE	NE	1.45 ± 0.18	0.18 ± 0.07	<0.001	<0.001
18-Hydroxy-eicosapentaenoic acid	18-HEPE	NE	1.51 ± 0.26	0.19 ± 0.11	<0.001	<0.001
LA metabolites						
9,10-Dihydroxy-octadecanoic acid	9,10-diHOME	P450	16.71 ± 6.03	7.38 ± 4.10	0.013	0.042
12,13-Epoxy-octadecanoic acid	12,13-EpOME	P450	12.65 ± 3.65	5.52 ± 2.11	0.002	0.012
12,13-Dihydroxy-octadecanoic acid	12,13-diHOME	P450	38.64 ± 13.16	10.86 ± 6.82	0.001	0.008
13-Hydroxy-octadecadienoic acid	13-HODE	NE	61.13 ± 20.15	23.91 ± 8.93	0.005	0.018

All values are picomoles per milliliter of plasma expressed as mean ± SD. MECH, mechanism.

The first and rate-limiting step of eicosanoid synthesis is the liberation of PUFAs from their esterified form in the sn-2 position of membrane phospholipids by cytosolic phospholipase. In our study, both the cytosolic (group IV) and secretory PLA2 were elevated with HFD and decreased with AICAR. Cytosolic PLA2 is essential for adipocyte differentiation in obesity models (40). Cytosolic PLA2 (group IV)-deficient mice are resistant to the hepatic effects of HFD due to the decrease in the production of downstream products, confirming the crucial role of this enzyme in high induced fat disease (41). Cytosolic PLA2 is also central to oxidative signaling in renal epithelial cells, releasing AA and its downstream products (42). Isoenzymes of PLA2 are differentially expressed in various tissues in response to inflammation; for example, expression of the group VII PLA2 gene is increased in the livers of Zucker obese rats, while expression of group IVA and VIA PLA2 was inhibited (43). PLA2 isoenzymes also demonstrate substrate selectivity to certain forms of phospholipids in membranes and specific PUFAs (44). Kidney desaturases and elongases that

TABLE 4. Eicosanoid metabolites altered with HFD in the venous circulation

Name	Acronym	MECH	STD	HFD	P	q Value
Up with HFD						
AA metabolites						
Arachidonic acid	AA	PUFA	7,763.6 ± 1,110.5	13,307.3 ± 2,881.1	0.001	0.009
8.9-Epoxyeicosatrienoic acid	8,9-EET	P450	0.04 ± 0.08	0.51 ± 0.41	0.012	0.049
5,6-Epoxyeicosatrienoic acid	5,6-EET	P450	8.26 ± 4.66	20.49 ± 6.51	0.006	0.031
11,12-Epoxyeicosatrienoic acid	11,12-EET	P450	1.82 ± 0.65	3.89 ± 0.97	0.002	0.015
6-Keto-prostaglandin $F_{1\alpha}$	6k-PGF$_{1\alpha}$	COX	1.11 ± 0.44	2.64 ± 1.14	0.005	0.027
Down with HFD						
DHA metabolites						
4-Hydroxy-docosahexaenoic acid	4-HDoHE	LOX	9.87 ± 2.09	3.26 ± 0.61	<0.001	0.001
20-Hydroxy-docosahexaenoic acid	20-HDoHE	NE	0.89 ± 0.33	0.13 ± 0.22	0.004	0.027
ALA metabolites						
9-Hydroxy-octatrienoic acid	9-HOTrE	LOX	1.87 ± 0.68	0.69 ± 0.21	0.001	0.007
EPA metabolites						
Eicosapentaenoic acid	EPA	PUFA	10,459.9 ± 4,175.6	4,259.2 ± 1,425.1	0.008	0.035
9-Hydroxy-eicosapentaenoic acid	9-HEPE	NE	4.50 ± 2.72	0.45 ± 0.60	0.009	0.037
11-Hydroxy-eicosapentaenoic acid	11-HEPE	NE	1.06 ± 0.22	0.21 ± 0.10	<0.001	0.001
18-Hydroxy-eicosapentaenoic acid	18-HEPE	NE	1.11 ± 0.22	0.14 ± 0.06	<0.001	0.001
12-Hydroxy-eicosapentaenoic acid	12-HEPE	LOX	42.94 ± 25.80	7.48 ± 9.07	0.005	0.028
5-Hydroxy-eicosapentaenoic acid	5-HEPE	LOX	2.25 ± 0.64	0.17 ± 0.11	<0.001	0.001
15-Hydroxy-eicosapentaenoic acid	15-HEPE	LOX	1.36 ± 0.74	0.07 ± 0.10	0.001	0.009
14(15)-Epoxyeicosatetraenoic acid	14,15-EpETE	P450	0.72 ± 0.23	0.18 ± 0.10	0.001	0.007

All values are picomoles per milliliter of plasma expressed as mean ± SD. MECH, mechanism.
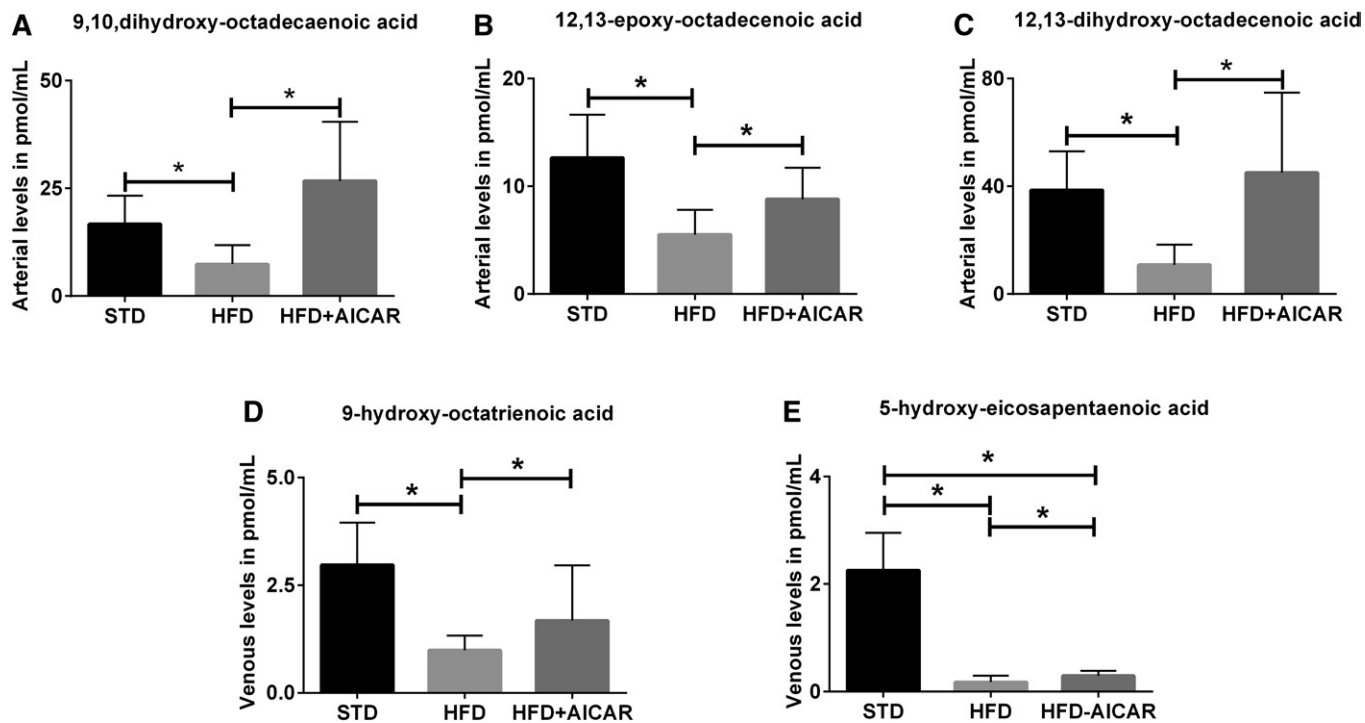
Fig. 5. Profile of eicosanoid species in the circulation regulated by HFD and AICAR (HFD+AICAR). Profile of eicosanoid species in arterial and venous circulation in mice fed a STD, HFD, or HFD with AICAR therapy. Values are expressed as mean ± SD (n = 6 in each group). Statistical analyses were performed by one-way ANOVA followed by Fisher post hoc tests. All *P* values corrected for Bonferroni FDR correction of *q ≤ 0.05. LA metabolites of P450 in the artery, 9,10-diHOME (A), 12,13-EpHOME (B), and 12,13-diHOME (C). Venous LOX metabolites of ALA, 9-HOTrE (D), and EPA, 5-HEPE (E).

are responsible for conversion between the various PUFAs are unaffected by HFD or AMPK activation in our study. However, livers of obese Zucker rats demonstrated increased expression of delta-6 desaturase and elongase-6 (43). Diets in the HFD and STD groups had similar *n-6* to *n-3* ratios, and the pattern in the circulation and the kidney do not reflect this ratio. AA is increased in the circulation, kidney, and urine with HFD in our study and this is consistent with increased circulating PUFAs demonstrated with HFD feeding in Sprague-Dawley rats (45). In excess nutrient states, phospholipase D suppresses AMPK activity through the mammalian/mechanistic target of rapamycin (mTOR); in return, AMPK activation decreased phospholipase D activity similar to the effect of AMPK activation on other phospholipases in vascular smooth muscles and endothelial cells (19, 46, 47). Thus, the effect of AMPK activation on phospholipases in our study could be responsible for the changes to the PUFA levels with AICAR therapy.

Both COX-1 and COX-2 and their downstream products, PGD_2, PGE_2, and PGI_2, are involved in renal vasodilation. PGE_2 is the central PG synthesized in the kidney tubules and mesangial cells, and activation of its receptors causes contraction of vascular muscle cells and increased calcium in mesangial cells and inhibits sodium reabsorption at the thick ascending limb of the loop of Henle (48). In our study, PGE_2 is decreased in the kidney with HFD, but its metabolites, PGA_2, PGB_2, and PGEM, are increased in the urine with HFD. PGI_2 metabolites, 6,15 dk-,dh-$PGF_{1\alpha}$ and 6k-PGE_1, are increased in the urine with HFD similar to the PGD_2 metabolites, PGJ_2 and dhkPGD_2. Urinary

AA-derived eicosanoids, primarily downstream of COX metabolite, PGH_2, were increased with HFD and decreased with AICAR therapy. Increased flux in these pathways possibly results in decreased bioavailability of the renal vasodilators. In line with our findings, COX-2 expression was increased in the renal cortex, blood vessels, and urine in obese Zucker rats (49). Increased urinary TXB_2 and 6-keto-$PGF_{1\alpha}$ and decreased PGE_2 excretion rates were evident in obese Zucker rats. Similarly, a decreased urinary PGI_2/TXA_2 ratio has been demonstrated in diabetic humans as well as in diabetic animal models. Rofecoxib, a COX-2 inhibitor, decreases vascular and glomerular damage when administered to obese Zucker rats (29). Decreased $PGF_{2\alpha}$ and 8-iso-$PGF_{2\alpha}$ levels contribute to the decreased glomerulosclerosis in obese Zucker rats treated with rofecoxib. COX-2 inhibition and decreases in 8-iso-$PGF_{2\alpha}$ levels have also been shown to ameliorate renal injury associated with hypertensive rats (50). This pattern is also reflected in the urinary levels of 8-iso-$PGF_{2\alpha}$ in our mouse model of HFD-induced kidney disease.

Renal P450 epoxidation generates EETs that are metabolized by soluble epoxide hydrolase (sEH) to less active dihydroxyeicosatrienoic acids. Decreased renal expression of CYP2C epoxygenase enzymes has been observed in diabetes, HFD-fed insulin resistance rats, and the kidney and mesenteric blood vessels of obese Zucker rats (51). Additionally, sEH expression is increased in blood vessels of obese rats and could further contribute to the decrease in EET bioavailability, implicating impaired endothelial dilator responses in obesity and diabetes. The cytokines, IL-6

Fig. 6. Schematic diagram of the eicosanoid metabolites regulated by AMPK activation to reverse the effects of HFD in the kidney, urine, and arterial and venous circulation. Adrenic acid metabolites, dihomo-PGF$_{2\alpha}$ and dihomo-15d-PGD$_2$; AA metabolites, PGEM and PGFM, and PGF$_{2\alpha}$; EPA metabolites, PGE$_3$, TXB$_3$, and 5-HEPE; ALA metabolite, 9-HOTrE; DHA metabolites, 19,20-DiHDPA, 16-HDoHE, 15(t)-PD$_1$, 7-HDoHE, 11-HDoHE, 8-HDoHE, and 13-HDoHE; and finally LA metabolites, 9,10-diHOME; 12,13-EpOME, and 12,13-diHOME. Red font indicates that HFD increases these metabolites and AICAR reverses them, while blue font indicates the metabolite is decreased with HFD and AICAR reverses this trend.

and TNF-α, decrease expression of P450 epoxygenase enzymes. TNF-α and EETs act via the NFκB pathway causing elevated MCP-1 levels that have been observed in HFD-induced kidney disease in mice (6). Obese Zucker rats have increased renal vascular CYP4A expression and increased generation of 20-HETE (49). However, renal tubular CYP4A expression was decreased in Sprague-Dawley rats on HFD (52). The AA metabolites, 20-HETE, EET, and dihydroxyeicosatrienoic acid, are decreased with HFD in the kidney and associated with the diet-induced change in blood pressure and renal function of Sprague-Dawley rats (52, 53). In our study, the kidney P450 products of AA, 9-HETE and EETs, are increased with HFD, just as many of the EETs are also increased in the circulation and urine. Pharmacological inhibition or transgenic deletion of sEH, the dominant enzyme in degrading EETs, has been shown to protect mice from various adverse effects induced by obesity (54). Thus, protective eicosanoid metabolites of AA-EET are increased with HFD in the kidney. In HFD-fed mice, plasma profiling revealed increases in circulating P450 metabolites of LA-EpOMEs (55), which is a different trend to the one observed in the

arterial circulation of our HFD mice maintained on HFD for a longer period.

Central adipose tissue in obese Zucker rats shows increased LOX expression along with inflammatory markers (56). 5-LOX products induce NF-κB expression and secretion of inflammatory cytokines like MCP-1, TNF-α, macrophage inflammatory protein-1γ, and IL-6 by the adipose tissue. The 5-LOX pathway plays a major role in obesity-induced fatty liver disease (57). In our study, LOX metabolites of AA and AA metabolites, 6(R),15(R)-LXA$_4$ and 6(S)-LXA$_4$, are increased in the kidney with HFD in our study, and LXA$_4$ has been shown by our group to attenuate inflammation in HFD-related kidney disease (10). Similarly, LOX metabolites of DHA-HDoHE were elevated in the kidney, whereas LOX metabolites of EPA-HEPEs were all decreased in the kidney and the circulation.

Omega 3 FA (DHA and EPA) supplementation in ob/ob mice induced AMPK phosphorylation and alleviated hepatic steatosis. Omega 3 supplementation is anti-inflammatory, promotes insulin sensitivity, and raises *n-3* FA-derived resolvins and protectins (58). Obesity significantly decreased DHA-derived 17-hydroxydocosahexaenoic acid (resolvin

TABLE 5. The trends in the kidney and urine of highly correlated metabolites using PC analysis

Variable	PC Variables	PC Variance	ANOVA P All	Post Hoc P STD versus HFD	Post Hoc P HFD versus HFD+AICAR
Kidney					
AA					
LOX	15	64.2	0.02	0.03[a]	1
COX	15	45.0	0.81	1	1
P450	17	49.7	0.09	0.11	1
13 PGR	2	60.6	0.06	0.11	1
NE	3	42.2	0.20	0.34	1
EPA					
LOX	3	93.0	0.00002	0.00008[b]	1
NE	2	77.9	0.0000003	0.000001[b]	1
DHA					
LOX	4	77.2	0.007	0.006[a]	0.28
COX	2	96.0	0.001	0.001[a]	0.03
P450	2	97.5	0.003	0.003[a]	0.08
NE	4	95.8	0.008	0.007[a]	0.12
DGLA					
LOX	2	92.5	0.03	0.06[b]	1
LA					
LOX	2	98.0	0.07	0.40	1
NE	2	77.4	0.06	0.42	1
ALA					
LOX	3	82.4	0.26	0.89	0.33
Urine					
AA					
LOX	28	46.3	0.06	0.42	0.95
COX	27	33.6	0.0005	0.004[a]	1
P450	19	53.9	0.12	0.70	1
13 PGR	3	47.7	0.03	0.04[b]	1
PGDH	5	45.6	0.00000002	0.00000001[a]	0.00003
NE	3	48.5	0.002	0.001[a]	0.09
EPA					
LOX	3	96.8	0.14	0.214	0.33
COX	5	50.8	0.00022	0.000161[b]	0.03[c]
CYP	2	82.0	0.85	1	1
NE	3	82.2	0.05	0.24	0.06
DHA					
LOX	6	55.0	0.49	0.94	1
COX	2	96.0	0.83	1	1
NE	4	71.3	0.85	1	1
DGLA					
LOX	2	97.1	0.02	0.03[a]	1
LA					
LOX	2	98.0	0.07	0.4	1
NE	2	77.4	0.04	0.36	0.72
ALA					
LOX	3	82.4	0.26	0.88	0.33
Adrenic acid					
COX	2	71.3	0.00002	0.00002[b]	0.006[c]

PC variables, number of eicosanoids in the PC; PC variance, amount of variance explained by the PC; ANOVA P, P generated comparing all three groups; HFD+AICAR, HFD and AICAR therapy; 13 PGR, delta13-15-ketoprostaglandin reductase; PGDH, 15-hydroxyprostaglandin dehydrogenase.

[a]Elevated with HFD.
[b]Decreased with HFD.
[c]Elevated with AICAR

D1 precursor) and PD_1 levels in murine adipose tissue. Notably, 17-hydroxydocosahexaenoic acid treatment reduced adipose tissue expression of inflammatory cytokines, increased adiponectin expression, and improved glucose tolerance parallel to insulin sensitivity in obese mice (59). A concentrated formulation of *n-3* PUFAs attenuates albuminuria, renal function, SREBP-1 expression, and triglyceride levels in the kidneys of type 2 diabetic obese db/db mice (60). DHA and DHA metabolites in the kidney, the various HDoHEs, EpDPE and DiHDPA produced by P450, LOX, and NE in the kidney are all increased with HFD in our study. While the kidney and urine DHA metabolites were increased, the circulatory DHA metabolites were decreased, suggesting local production in the kidney. With HFD exposure, the DHA metabolites, $15(t)-PD_1$ and PDX, are both increased in the kidney and urine, respectively. In our study, HEPEs derived from the n-3 EPA were all decreased in the kidney, urine, and circulation. The EPA metabolite, PGH_3, and its hydroxyl metabolites were all decreased in the circulation with HFD. Downregulation of HEPEs in our study represents suppression of anti-inflammatory signals.

TABLE 6. The trends in the arterial and venous blood of highly correlated metabolites using PC analysis

			ANOVA P	Post Hoc P	
Variable	PC Variables	PC Variance	All	STD versus HFD	HFD versus HFD+AICAR
Artery					
AA					
LOX	9	40.9	0.73	1	1
13 PGR	2	70.3	0.42	0.60	1
COX	6	59.9	0.90	1	1
P450	13	49.3	0.13	0.43	0.16
EPA					
LOX	3	78.9	0.000003	0.00004[a]	0.72
DHA					
LOX	2	79.9	0.001	0.003[a]	1
P450	2	78.1	0.01	0.03[a]	1
NE	4	77.1	0.01	0.01[a]	1
LA					
NE	2	92.8	0.32	0.43	0.97
ALA					
LOX	3	75.7	0.04	0.03[a]	0.37
Vein					
AA					
LOX	8	59.4	0.87	1	1
13 PGR	2	50.5	0.06	0.06	0.47
COX	5	67.2	0.84	1	1
P450	15	47.9	0.12	1	0.19
EPA					
LOX	3	78.0	0.00002	0.00003[a]	0.60
NE	2	82.4	0.00004	0.0003[a]	1
DHA					
LOX	3	58.0	0.0004	0.002[a]	1
NE	3	73.9	0.08	0.09	0.76
LA					
NE	2	90.4	0.11	0.79	0.11
ALA					
LOX	3	73.7	0.02	0.03[a]	0.09

PC variables, number of eicosanoids in the PC; PC variance, amount of variance explained by the PC; ANOVA P, P generated comparing all three groups; HFD+AICAR, high-fat diet and AICAR therapy; 13 PGR, delta13-15-ketoprostaglandin reductase; PGDH, 15-hydroxyprostaglandin dehydrogenase.
[a]Decreased with HFD.

AMPK is a nutrient sensor and is inhibited by nutrient excess states. In our prior studies, the effects of HFD-induced kidney disease were reversed with AMPK activation with AICAR therapy. AMPK activation reversed the inflammatory profile, lipid accumulation, and low adiponectin levels that were caused by HFD (9, 10, 61). Diet reversal alone was unable to improve the renal inflammation and apoptosis in HFD-induced kidney damage, emphasizing the persistence of renal injury even after 8 weeks of dietary control (62). However, AMPK activation with metformin treatment was able to reduce the levels of inflammatory and apoptotic markers that remain residual despite diet reversal. Also, metformin ameliorated HFD-induced glomerular injury, renal fatty acid oxidation, and serum adipokine levels (62–64). Metformin reduces fat content by decreasing SREBP-1, FAS, and ACC expression in the kidney (65). In our study, AICAR reversed the upregulation of phospholipase and free PUFAs. The influence of AICAR is evident in reversing the increased hydroxyl DHA metabolites in the kidney and COX metabolites of AA in the urine. In the venous circulation, AICAR reverses the downregulation of the P450 metabolite of LA, 9-HOTrE, and the LOX metabolite of LA, 5-HEPE. HFD has been previously shown to increase leukotoxins, such as EpOMEs; while in our study, EpOME metabolites are decreased (55). AICAR also reverses the downregulation of 9,10-diHOME, 12,13-diHOME, and 12,13-EpOME in the arterial circulation in our study. Thus, AMPK activation is able to reverse key pathways in eicosanoid metabolism and helps to ameliorate changes resulting from HFD.

In this current study, we demonstrate modulation of PUFAs and their metabolites after HFD as well as AMPK activation in the kidney, but we cannot delineate the origin of the various eicosanoids in the circulation and urine, which could be from the diet, liver, muscle, pancreas, and/or gut microbiota. Again, the changes in the eicosanoids might be influenced by the upstream action of phospholipases on specific PUFAs whose pattern might be reflective of the specific diet; although both of the diets had a similar n-6:n-3 ratio, the specific composition of HFD might have influenced the eicosanoid changes. Also, as the influence of AICAR is not restricted to one specific oxygenase or PUFA, its influence on phospholipases might influence its action to follow the pattern of the predominant PUFA availability in various compartments. Though we have independently demonstrated the effects of HFD on the kidney pathology and the lipid and inflammatory profile, we cannot conclusively provide evidence that the eicosanoid changes are the sole cause of HFD-induced kidney disease or the reason for the AICAR-induced amelioration. Also,

the eicosanoids might have differential changes based on temporal exposure to HFD, and this was not conclusively studied in this work. It is also difficult to tease out the source of inflammation in such models, as both HFD and AICAR therapy, in addition to altering inflammation, also influence body weight. Another factor to account for is that pharmacologic AMPK inhibition might not be complete, and genetic manipulation of AMPK might provide a clearer picture. Genetic manipulation of the pathways clearly influenced by AMPK will help us to study downstream and upstream changes and their interaction with the eicosanoid pathways and link them to renal pathology.

In summary, in this study using a targeted lipidomic approach, we demonstrate the dysregulation of eicosanoid synthesis and metabolism in the kidney with HFD and its amelioration with AMPK activation. Our work sheds light on the mechanism behind HFD-related toxicity and the eicosanoid pathways under the control of AMPK activation in the kidney. We also expose the various pro- and anti-inflammatory mechanisms in HFD-mediated kidney disease that are altered with AMPK activation. Future studies that manipulate these dysregulated pathways might open therapeutic avenues in the management of high-fat-induced kidney disease.

REFERENCES

1. Ogden, C. L., M. D. Carroll, C. D. Fryar, and K. M. Flegal. 2015. Prevalence of obesity among adults and youth: United States, 2011–2014. *NCHS Data Brief.* **219:** 1–8.
2. Mathew, A. V., S. Okada, and K. Sharma. 2011. Obesity related kidney disease. *Curr. Diabetes Rev.* **7:** 41–49.
3. Bruce, K. D., and C. D. Byrne. 2009. The metabolic syndrome: common origins of a multifactorial disorder. *Postgrad. Med. J.* **85:** 614–621.
4. de Vries, A. P., P. Ruggenenti, X. Z. Ruan, M. Praga, J. M. Cruzado, I. M. Bajema, V. D. D'Agati, H. J. Lamb, D. Pongrac Barlovic, R. Hojs, et al. 2014. Fatty kidney: emerging role of ectopic lipid in obesity-related renal disease. *Lancet Diabetes Endocrinol.* **2:** 417–426.
5. Lin, J., T. T. Fung, F. B. Hu, and G. C. Curhan. 2011. Association of dietary patterns with albuminuria and kidney function decline in older white women: a subgroup analysis from the Nurses' Health Study. *Am. J. Kidney Dis.* **57:** 245–254.
6. Declèves, A. E., A. V. Mathew, R. Cunard, and K. Sharma. 2011. AMPK mediates the initiation of kidney disease induced by a high-fat diet. *J. Am. Soc. Nephrol.* **22:** 1846–1855.
7. Declèves, A. E., Z. Zolkipli, J. Satriano, L. Wang, T. Nakayama, M. Rogac, T. P. Le, J. L. Nortier, M. G. Farquhar, R. K. Naviaux, et al. 2014. Regulation of lipid accumulation by AMK-activated kinase in high fat diet-induced kidney injury. *Kidney Int.* **85:** 611–623.
8. Yamamoto, T., Y. Takabatake, A. Takahashi, T. Kimura, T. Namba, J. Matsuda, S. Minami, J. Y. Kaimori, I. Matsui, T. Matsusaka, et al. 2017. High-fat diet-induced lysosomal dysfunction and impaired autophagic flux contribute to lipotoxicity in the kidney. *J. Am. Soc. Nephrol.* **28:** 1534–1551.
9. Börgeson, E., V. Wallenius, G. H. Syed, M. Darshi, J. Lantero Rodriguez, C. Biorserud, M. Ragnmark Ek, P. Bjorklund, M. Quiding-Jarbrink, L. Fandriks, et al. 2017. AICAR ameliorates high-fat diet-associated pathophysiology in mouse and ex vivo models, independent of adiponectin. *Diabetologia.* **60:** 729–739.
10. Börgeson, E., A. M. F. Johnson, Y. S. Lee, A. Till, G. H. Syed, S. T. Ali-Shah, P. J. Guiry, J. Dalli, R. A. Colas, C. N. Serhan, et al. 2015. Lipoxin A(4) attenuates obesity-induced adipose inflammation and associated liver and kidney disease. *Cell Metab.* **22:** 125–137.
11. van der Heijden, R. A., J. Bijzet, W. C. Meijers, G. K. Yakala, R. Kleemann, T. Q. Nguyen, R. A. de Boer, C. G. Schalkwijk, B. P. C. Hazenberg, U. J. F. Tietge, et al. 2015. Obesity-induced chronic inflammation in high fat diet challenged C57BL/6J mice is associated with acceleration of age-dependent renal amyloidosis. *Sci. Rep.* **5:** 16474.
12. Altunkaynak, M. E., E. Özbek, B. Z. Altunkaynak, İ. Can, D. Unal, and B. Unal. 2008. The effects of high-fat diet on the renal structure and morphometric parametric of kidneys in rats. *J. Anat.* **212:** 845–852.
13. Barcelli, U. O., D. C. Beach, B. Thompson, M. Weiss, and V. E. Pollak. 1988. A diet containing n-3 and n-6 fatty acids favorably alters the renal phospholipids, eicosanoid synthesis and plasma lipids in nephrotic rats. *Lipids.* **23:** 1059–1063.
14. Nakamura, M. T., and T. Y. Nara. 2003. Essential fatty acid synthesis and its regulation in mammals. *Prostaglandins Leukot. Essent. Fatty Acids.* **68:** 145–150.
15. Schmitz, G., and J. Ecker. 2008. The opposing effects of n-3 and n-6 fatty acids. *Prog. Lipid Res.* **47:** 147–155.
16. Carling, D. 2004. The AMP-activated protein kinase cascade–a unifying system for energy control. *Trends Biochem. Sci.* **29:** 18–24.
17. Corton, J. M., J. G. Gillespie, S. A. Hawley, and D. G. Hardie. 1995. 5-Aminoimidazole-4-carboxamide ribonucleoside. A specific method for activating AMP-activated protein kinase in intact cells? *Eur. J. Biochem.* **229:** 558–565.
18. Hardie, D. G., S. A. Hawley, and J. W. Scott. 2006. AMP-activated protein kinase–development of the energy sensor concept. *J. Physiol.* **574:** 7–15.
19. El Hadri, K., C. Denoyelle, L. Ravaux, B. Viollet, M. Foretz, B. Friguet, M. Rouis, and M. Raymondjean. 2015. AMPK signaling involvement for the repression of the IL-1β-induced group IIA secretory phospholipase A2 expression in VSMCs. *PLoS One.* **10:** e0132498.
20. Jiang, S., H. Chen, Z. Wang, J. J. Riethoven, Y. Xia, J. Miner, and M. Fromm. 2011. Activated AMPK and prostaglandins are involved in the response to conjugated linoleic acid and are sufficient to cause lipid reductions in adipocytes. *J. Nutr. Biochem.* **22:** 656–664.
21. Namgaladze, D., R. G. Snodgrass, C. Angioni, N. Grossmann, N. Dehne, G. Geisslinger, and B. Brüne. 2015. AMP-activated protein kinase suppresses arachidonate 15-lipoxygenase expression in interleukin 4-polarized human macrophages. *J. Biol. Chem.* **290:** 24484–24494.
22. Quehenberger, O., A. M. Armando, and E. A. Dennis. 2011. High sensitivity quantitative lipidomics analysis of fatty acids in biological samples by gas chromatography-mass spectrometry. *Biochim. Biophys. Acta.* **1811:** 648–656.
23. Quehenberger, O., A. M. Armando, A. H. Brown, S. B. Milne, D. S. Myers, A. H. Merrill, S. Bandyopadhyay, K. N. Jones, S. Kelly, R. L. Shaner, et al. 2010. Lipidomics reveals a remarkable diversity of lipids in human plasma. *J. Lipid Res.* **51:** 3299–3305.
24. Dumlao, D. S., M. W. Buczynski, P. C. Norris, R. Harkewicz, and E. A. Dennis. 2011. High-throughput lipidomic analysis of fatty acid derived eicosanoids and N-acylethanolamines. *Biochim. Biophys. Acta.* **1811:** 724–736.
25. Xia, J., and D. S. Wishart. 2002. Using MetaboAnalyst 3.0 for comprehensive metabolomics data analysis. *Curr. Protoc. Bioinformatics.* **55:** 14.10.1–14.10.91.
26. Afshinnia, F., L. Zeng, J. Byun, S. Wernisch, R. Deo, J. Chen, L. Hamm, E. R. Miller, E. P. Rhee, M. J. Fischer, et al. Elevated lipoxygenase and cytochrome P450 products predict progression of chronic kidney disease. *Nephrol. Dial. Transplant.* Epub ahead of print. July 25, 2018; doi:10.1093/ndt/gfy232.
27. Matsuda, M., T. Kawamoto, and R. Tamura. 2017. Predictive value of serum dihomo-gamma-linolenic acid level and estimated Delta-5 desaturase activity in patients with hepatic steatosis. *Obes. Res. Clin. Pract.* **11:** 34–43.
28. Li, S., Q. Chu, J. Ma, Y. Sun, T. Tao, R. Huang, Y. Liao, J. Yue, J. Zheng, L. Wang, et al. 2017. Discovery of novel lipid profiles in PCOS: do insulin and androgen oppositely regulate bioactive lipid production? *J. Clin. Endocrinol. Metab.* **102:** 810–821.
29. Dey, A., C. Maric, W. H. Kaesemeyer, C. Z. Zaharis, J. Stewart, J. S. Pollock, and J. D. Imig. 2004. Rofecoxib decreases renal injury in obese Zucker rats. *Clin. Sci. (Lond.).* **107:** 561–570.
30. Mure, K., N. Yoshimura, M. Hashimoto, S. Muraki, H. Oka, S. Tanaka, H. Kawaguchi, K. Nakamura, T. Akune, and T. Takeshita. 2015. Urinary 8-iso-prostaglandin F2alpha as a marker of metabolic risks in the general Japanese population: The ROAD study. *Obesity (Silver Spring).* **23:** 1517–1524.
31. Yu, D., Z. Xu, X. Yin, F. Zheng, X. Lin, Q. Pan, and H. Li. 2015. Inverse relationship between serum lipoxin A4 level and the risk of metabolic syndrome in a middle-aged Chinese population. *PLoS One.* **10:** e0142848.

32. Chen, H. M., Z. H. Liu, C. H. Zeng, S. J. Li, Q. W. Wang, and L. S. Li. 2006. Podocyte lesions in patients with obesity-related glomerulopathy. *Am. J. Kidney Dis.* **48:** 772–779.

33. Kambham, N., G. S. Markowitz, A. M. Valeri, J. Lin, and V. D. D'Agati. 2001. Obesity-related glomerulopathy: an emerging epidemic. *Kidney Int.* **59:** 1498–1509.

34. Mima, A., T. Yasuzawa, G. L. King, and S. Ueshima. 2018. Obesity-associated glomerular inflammation increases albuminuria without renal histological changes. *FEBS Open Bio.* **8:** 664–670.

35. Jiang, T., Z. Wang, G. Proctor, S. Moskowitz, S. E. Liebman, T. Rogers, M. S. Lucia, J. Li, and M. Levi. 2005. Diet-induced obesity in C57BL/6J mice causes increased renal lipid accumulation and glomerulosclerosis via a sterol regulatory element-binding protein-1c-dependent pathway. *J. Biol. Chem.* **280:** 32317–32325.

36. Kume, S., T. Uzu, S. Araki, T. Sugimoto, K. Isshiki, M. Chin-Kanasaki, M. Sakaguchi, N. Kubota, Y. Terauchi, T. Kadowaki, et al. 2007. Role of altered renal lipid metabolism in the development of renal injury induced by a high-fat diet. *J. Am. Soc. Nephrol.* **18:** 2715–2723.

37. Rampanelli, E., P. Ochodnicky, J. P. Vissers, L. M. Butter, N. Claessen, A. Calcagni, L. Kors, L. A. Gethings, S. J. Bakker, M. H. de Borst, et al. 2018. Excessive dietary lipid intake provokes an acquired form of lysosomal lipid storage disease in the kidney. *J. Pathol.* **246:** 470–484.

38. D'Agati, V. D., A. Chagnac, A. P. de Vries, M. Levi, E. Porrini, M. Herman-Edelstein, and M. Praga. 2016. Obesity-related glomerulopathy: clinical and pathologic characteristics and pathogenesis. *Nat. Rev. Nephrol.* **12:** 453–471.

39. Bakker, P. J., L. M. Butter, L. Kors, G. J. Teske, J. Aten, F. S. Sutterwala, S. Florquin, and J. C. Leemans. 2014. Nlrp3 is a key modulator of diet-induced nephropathy and renal cholesterol accumulation. *Kidney Int.* **85:** 1112–1122.

40. Peña, L., C. Meana, A. M. Astudillo, G. Lorden, M. Valdearcos, H. Sato, M. Murakami, J. Balsinde, and M. A. Balboa. 2016. Critical role for cytosolic group IVA phospholipase A2 in early adipocyte differentiation and obesity. *Biochim. Biophys. Acta.* **1861:** 1083–1095.

41. Ii, H., N. Yokoyama, S. Yoshida, K. Tsutsumi, S. Hatakeyama, T. Sato, K. Ishihara, and S. Akiba. 2009. Alleviation of high-fat diet-induced fatty liver damage in group IVA phospholipase A2-knockout mice. *PLoS One.* **4:** e8089.

42. Cui, X-L., Y. Ding, L. D. Alexander, C. Bao, O. K. Al-Khalili, M. Simonson, D. C. Eaton, and J. G. Douglas. 2006. Oxidative signaling in renal epithelium: critical role of cytosolic phospholipase A2 and p38(SAPK). *Free Radic. Biol. Med.* **41:** 213–221.

43. Fèvre, C., S. Bellenger, A. S. Pierre, M. Minville, J. Bellenger, J. Gresti, M. Rialland, M. Narce, and C. Tessier. 2011. The metabolic cascade leading to eicosanoid precursors–desaturases, elongases, and phospholipases A2–is altered in Zucker fatty rats. *Biochim. Biophys. Acta.* **1811:** 409–417.

44. Diez, E., F. H. Chilton, G. Stroup, R. J. Mayer, J. D. Winkler, and A. N. Fonteh. 1994. Fatty acid and phospholipid selectivity of different phospholipase A2 enzymes studied by using a mammalian membrane as substrate. *Biochem. J.* **301:** 721–726.

45. Liu, T-W., T. D. Heden, E. M. Morris, K. L. Fritsche, V. J. Vieira-Potter, and J. P. Thyfault. 2015. High-fat diet alters serum fatty acid profiles in obesity prone rats: implications for in-vitro studies. *Lipids.* **50:** 997–1008.

46. Mukhopadhyay, S., M. Saqcena, A. Chatterjee, A. Garcia, M. A. Frias, and D. A. Foster. 2015. Reciprocal regulation of AMP-activated protein kinase and phospholipase D. *J. Biol. Chem.* **290:** 6986–6993.

47. Yang, L., H-L. Cong, S-F. Wang, and T. Liu. 2017. AMP-activated protein kinase mediates the effects of lipoprotein-associated phospholipase A2 on endothelial dysfunction in atherosclerosis. *Exp. Ther. Med.* **13:** 1622–1629.

48. Breyer, M. D., Y. Zhang, Y. F. Guan, C. M. Hao, R. L. Hebert, and R. M. Breyer. 1998. Regulation of renal function by prostaglandin E receptors. *Kidney Int. Suppl.* **67:** S88–S94.

49. Dey, A., R. S. Williams, D. M. Pollock, D. W. Stepp, J. W. Newman, B. D. Hammock, and J. D. Imig. 2004. Altered kidney CYP2C and cyclooxygenase-2 levels are associated with obesity-related albuminuria. *Obes. Res.* **12:** 1278–1289.

50. Tomida, T., Y. Numaguchi, Y. Nishimoto, M. Tsuzuki, Y. Hayashi, H. Imai, H. Matsui, and K. Okumura. 2003. Inhibition of COX-2 prevents hypertension and proteinuria associated with a decrease of 8-iso-PGF2alpha formation in L-NAME-treated rats. *J. Hypertens.* **21:** 601–609.

51. Zhao, X., A. Dey, O. P. Romanko, D. W. Stepp, M. H. Wang, Y. Zhou, L. Jin, J. S. Pollock, R. C. Webb, and J. D. Imig. 2005. Decreased epoxygenase and increased epoxide hydrolase expression in the mesenteric artery of obese Zucker rats. *Am. J. Physiol. Regul. Integr. Comp. Physiol.* **288:** R188–R196.

52. Wang, M. H., A. Smith, Y. Zhou, H. H. Chang, S. Lin, X. Zhao, J. D. Imig, and A. M. Dorrance. 2003. Downregulation of renal CYP-derived eicosanoid synthesis in rats with diet-induced hypertension. *Hypertension.* **42:** 594–599.

53. Zhou, Y., S. Lin, H-H. Chang, J. Du, Z. Dong, A. M. Dorrance, M. W. Brands, and M-H. Wang. 2005. Gender differences of renal CYP-derived eicosanoid synthesis in rats fed a high-fat diet. *Am. J. Hypertens.* **18:** 530–537.

54. Iyer, A., K. Kauter, M. A. Alam, S. H. Hwang, C. Morisseau, B. D. Hammock, and L. Brown. 2012. Pharmacological inhibition of soluble epoxide hydrolase ameliorates diet-induced metabolic syndrome in rats. *Exp. Diabetes Res.* **2012:** 758614.

55. Wang, W., J. Yang, H. Yang, K. Z. Sanidad, B. D. Hammock, D. Kim, and G. Zhang. 2016. Effects of high-fat diet on plasma profiles of eicosanoid metabolites in mice. *Prostaglandins Other Lipid Mediat.* **127:** 9–13.

56. Chakrabarti, S. K., Y. Wen, A. D. Dobrian, B. K. Cole, Q. Ma, H. Pei, M. D. Williams, M. H. Bevard, G. E. Vandenhoff, S. R. Keller, et al. 2011. Evidence for activation of inflammatory lipoxygenase pathways in visceral adipose tissue of obese Zucker rats. *Am. J. Physiol. Endocrinol. Metab.* **300:** E175–E187.

57. Martínez-Clemente, M., J. Clària, and E. Titos. 2011. The 5-lipoxygenase/leukotriene pathway in obesity, insulin resistance, and fatty liver disease. *Curr. Opin. Clin. Nutr. Metab. Care.* **14:** 347–353.

58. González-Périz, A., R. Horrillo, N. Ferre, K. Gronert, B. Dong, E. Moran-Salvador, E. Titos, M. Martinez-Clemente, M. Lopez-Parra, V. Arroyo, et al. 2009. Obesity-induced insulin resistance and hepatic steatosis are alleviated by omega-3 fatty acids: a role for resolvins and protectins. *FASEB J.* **23:** 1946–1957.

59. Neuhofer, A., M. Zeyda, D. Mascher, B. K. Itariu, I. Murano, L. Leitner, E. E. Hochbrugger, P. Fraisl, S. Cinti, C. N. Serhan, et al. 2013. Impaired local production of proresolving lipid mediators in obesity and 17-HDHA as a potential treatment for obesity-associated inflammation. *Diabetes.* **62:** 1945–1956.

60. Katakura, M., M. Hashimoto, T. Inoue, A. Al Mamun, Y. Tanabe, R. Iwamoto, M. Arita, S. Tsuchikura, and O. Shido. 2014. Omega-3 fatty acids protect renal functions by increasing docosahexaenoic acid-derived metabolite levels in SHR.Cg-Lepr(cp)/NDmcr rats, a metabolic syndrome model. *Molecules.* **19:** 3247–3263.

61. Sharma, K., S. Ramachandrarao, G. Qiu, H. K. Usui, Y. Zhu, S. R. Dunn, R. Ouedraogo, K. Hough, P. McCue, L. Chan, et al. 2008. Adiponectin regulates albuminuria and podocyte function in mice. *J. Clin. Invest.* **118:** 1645–1656.

62. Tikoo, K., E. Sharma, V. R. Amara, H. Pamulapati, and V. S. Dhawale. 2016. Metformin improves metabolic memory in high fat diet (HFD)-induced renal dysfunction. *J. Biol. Chem.* **291:** 21848–21856.

63. Kim, D., J. E. Lee, Y. J. Jung, A. S. Lee, S. Lee, S. K. Park, S. H. Kim, B. H. Park, W. Kim, and K. P. Kang. 2013. Metformin decreases high-fat diet-induced renal injury by regulating the expression of adipokines and the renal AMP-activated protein kinase/acetyl-CoA carboxylase pathway in mice. *Int. J. Mol. Med.* **32:** 1293–1302.

64. Mount, P., M. Davies, S. W. Choy, N. Cook, and D. Power. 2015. Obesity-related chronic kidney disease-the role of lipid metabolism. *Metabolites.* **5:** 720–732.

65. Wang, W., X. H. Guo, H. H. Wu, N. H. Wang, and X. S. Xu. 2006. Effect of fenofibrate and metformin on lipotoxicity in OLETF rat kidney. [Article in Chinese] *Beijing Da Xue Xue Bao Yi Xue Ban.* **38:** 170–175.